Shielding of Magnetic Field Effects on Operators Working a Power Transmission Lines Using 3-D FEM

Padej Pao-la-or and Arak Bunmat
School of Electrical Engineering, Suranaree University of Technology, Nakhon Ratchasima, Thailand
Email: padej@sut.ac.th; arak.bunmat@gmail.com

***Abstract*— Inspection, maintenance, and repair of electric power transmission line systems is a core function of the electrical engineer, who does such work on a daily basis for electrical power distribution systems in all regions. In Thailand, this task is the responsibility of the Provincial Electricity Authority (PEA). This article proposes a mathematical model of the magnetic field around a 115 kV power transmission line hung over another 22 kV line on which the staffs are performing work. This was modelled using a 3-dimensional finite element model. It is to be used as a diagnostic tool for predicting the magnetic fields around power distribution cables. This study focused on shielding magnetic devices from electricity to reduce the negative effects of magnetic induction on workers maintaining 22 kV transmission lines. The current study reports the results of decreased use of magnetic materials to reduce the magnetic field and the effects of magnetic fields on human beings according to ICNIRP standards.**

***Index Terms*— transmission line, 3-D finite element method (3-D FEM), magnetic field, material shielding**

I. Introduction

Inspection, maintenance, and repair of electric transmission lines are the regular duties of engineers and electrical personnel. A 115kV power transmission line of the Provincial Electricity Authority (PEA) hung over a 22 kV power distribution line on the same tower was selected as a test stand in Nakhon Ratchasima province, Thailand. Generally, a transmission line will be disconnected while it is repaired and the current in the top transmission line continues to flow. This should be safe for personnel to perform duties. But in reality, there is an effect of the current and voltage of the transmission system overhead upon the operator. Magnetic fields are induced in the lower transmission line even though power is not being supplied to this line. As a result, personnel working in the distribution system can be harmed. Therefore, this article demonstrates how to reduce the magnetic field affecting the operator of the power transmission line with materials that reduce magnetic field problems and their associated hazards.

Normally this phenomenon can be explained in the form of a differential equation or integral equation where is difficult to find an exact solution. Therefore, it is necessary to use an approximate numerical solution. Numerical computations can quickly solve these partial differential equations [1]. The most effective and popular methods today include finite element methods. This research, in particular, requires the use of a 3-D finite element method. Finite element methods are numerical methods that are used to calculate the approximate solution of a problem in the form of a partial differential equation by dividing the scope of the problem into small elements.

We then construct the equations of each element in accordance with the differential equations, and the elements are connected by their adjacent nodes, which are the positions where the solutions are calculated. For the finite element method in this research, the 3-dimensional calculation of the finite element method was done by dividing the volume of the problem into many regions, the so-called elements. The displacement and force within each element at the boundaries shared with adjacent elements must be compatible and balanced. These shape and size of these elements depend on the resolution of each task, how much the shape needs to resemble the original. This elements, if considered in 3-D, may be tetrahedral hexahedrons, octahedrons, or pyramids, in which tetrahedra are used. This is because these shapes have the fewest nodes or junctions. Also, the tetrahedra can be assembled to form any other shape. The accuracy of the solution will depend on the size and number of elements used to solve the problem [2]-[5]. All the programming instructions were coded in the MATLAB environment. Moreover, due to excessive magnetic fields that might be harmful to people or livestock living nearby, careful investigation of the magnetic phenomena was done. According to the standards of the International Commission on Non-Ionizing Radiation Protection (ICNIRP), satisfactory simulation results also comply with the ICNIRP standard.

II. Magnetic Field Modeling for a Power Transmission

Mathematical models of magnetic fields (**B**) generated by high currents are expressed in terms of the intensity of the magnetic field (**H**) in which $\mathbf{B} = \mu\mathbf{H}$. The Helmholtz

Manuscript received July 24, 2018; revised July 7, 2019.

doi: 10.18178/ijmerr.8.5.779-785

equation is shown as (1) [6]-[7]. The magnetic field modeling follows Ampere's circuital law as follows:

$$\frac{\partial^2 \mathbf{H}}{\partial x^2}+\frac{\partial^2 \mathbf{H}}{\partial y^2}+\frac{\partial^2 \mathbf{H}}{\partial z^2}-\varepsilon\mu\frac{\partial^2 \mathbf{H}}{\partial t^2}-\mu\sigma\frac{\partial \mathbf{H}}{\partial t}=0 \quad (1)$$

where **H** is the intensity of a magnetic field, ε is the constant dielectric permittivity, t is the time, μ is the magnetic permeability, and σ is the conductivity. This paper considered the time-harmonic system by representing $\mathbf{H}=He^{j\omega t}$ [8], therefore

$$\frac{\partial \mathbf{H}}{\partial t}=j\omega H \quad \text{and} \quad \frac{\partial^2 \mathbf{H}}{\partial t^2}=-\omega^2 H$$

where ω is the angular frequency.

Therefore, (1) can be rewritten as:

$$\nabla^2 H-j\omega\sigma\mu H+\omega^2\varepsilon\mu H=0$$

Considering the problem in three dimensional *(x,y,z)* space, then

$$\frac{\partial}{\partial x}\left(\frac{\partial H}{\partial x}\right)+\frac{\partial}{\partial y}\left(\frac{\partial H}{\partial y}\right)+\frac{\partial}{\partial z}\left(\frac{\partial H}{\partial z}\right)-\left(j\omega\mu\sigma-\mu\varepsilon\omega^2\right)H=0 \quad (2)$$

As can be seen, to obtain an exact solution of (2) is difficult. In this paper, the FEM was employed to find an approximate solution to these equations.

III. FEM FOR THE TRANSMISSION LINE

A. Discretization

In this study, a 115 kV power transmission system was installed over the transmission line of a 22 kV distribution system of the Provincial Electricity Authority in Nakhon Ratchasima, as shown in Fig. 1. The modelling of this study was conducted in 3-D. The sizing was varied according to the need to analyze areas of interest within different parts of the system. Fig. 2 shows a 115 kV transmission line over a 22 kV system. Fig. 3 shows a human form.

The 3D-FEM domain of study can be discretized using linear tetrahedral elements. A tetrahedron consist of a single volume with 4 nodes, which can be done using SolidWorks 3-D in the grid generation mode. Fig. 4 displays the grid representation of the test system with 58,841nodes and 345,673 elements used to model a 22 kV power line.

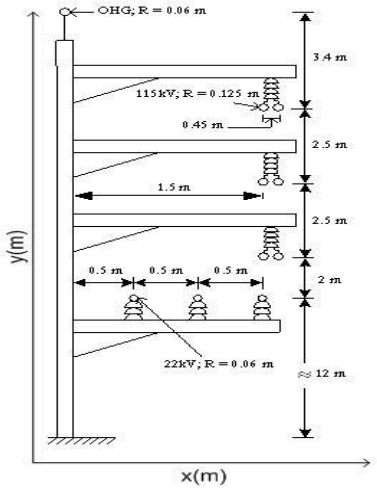

Figure 1. Details of the power lines

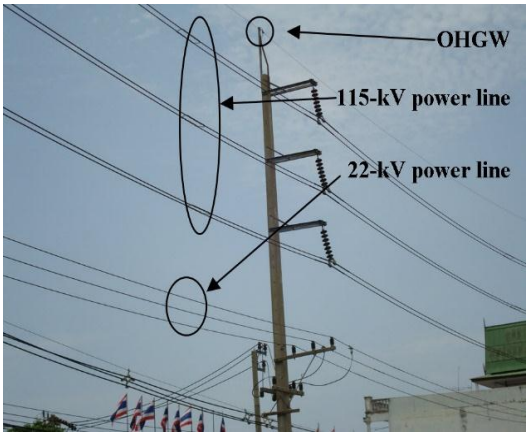

Figure 2. Power lines in Nakhon Ratchasima province modelled in the current study

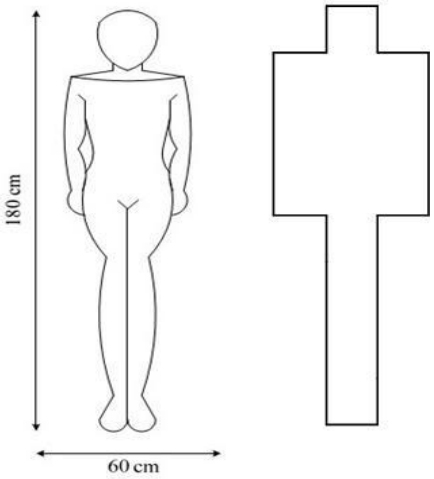

Figure 3. Detail of the human form

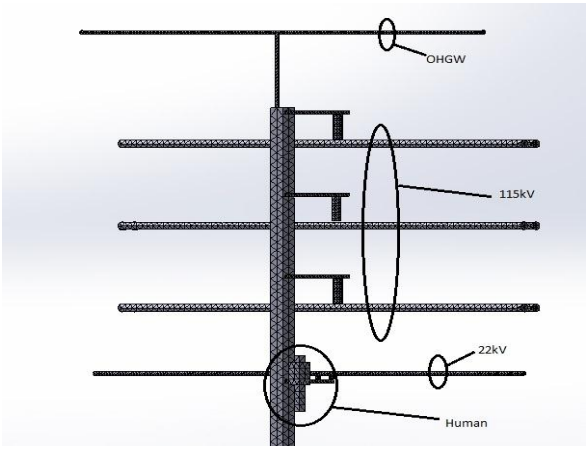

Figure 4. Mesh of power transmission line with a person working on a 22 kV line.

B. Finite Element Formulation

Equations of each component were derived directly from Maxwell's equations using a weighted residual method, where the weighting function was the same as the shape function. [9] - [10] According to this method, the magnetic field is shown as

$$H(x,y,z) = H_1N_1 + H_2N_2 + H_3N_3 + H_4N_4 \quad (3)$$

where N_n , $n = 1,2,3,4$ is the element shape function and the H_n , $n = 1,2,3,4$ is an approximation of the magnetic field intensity at each node (*1, 2, 3, 4*) of the elements, which is

$$N_n = \frac{1}{6V}(a_i + b_i x + c_i y + d_i z) \quad (4)$$

where V is the volume of the tetrahedral elements and,

$$a_1 = x_4(y_2z_3 - y_3z_2) + x_3(y_4z_2 - y_2z_4) + x_2(y_3z_4 - y_4z_3)$$
$$a_2 = x_4(y_3z_1 - y_1z_3) + x_3(y_1z_4 - y_4z_1) + x_1(y_4z_3 - y_3z_4)$$
$$a_3 = x_4(y_1z_2 - y_2z_1) + x_2(y_4z_1 - y_1z_4) + x_1(y_2z_4 - y_4z_2)$$
$$a_4 = x_3(y_2z_1 - y_1z_2) + x_2(y_1z_3 - y_3z_1) + x_1(y_3z_2 - y_2z_3)$$
$$b_1 = y_4(z_3 - z_2) + y_3(z_2 - z_4) + y_2(z_4 - z_3)$$
$$b_2 = y_4(z_3 - z_2) + y_1(z_3 - z_4) + y_3(z_4 - z_1)$$
$$b_3 = y_4(z_3 - z_2) + y_2(z_1 - z_4) + y_1(z_4 - z_2)$$
$$b_4 = y_3(z_3 - z_2) + y_1(z_2 - z_3) + y_2(z_3 - z_1)$$
$$c_1 = x_4(z_2 - z_3) + x_2(z_3 - z_4) + x_3(z_4 - z_2)$$
$$c_2 = x_4(z_3 - z_1) + x_3(z_1 - z_4) + x_1(z_4 - z_3)$$
$$c_3 = x_4(z_1 - z_2) + x_1(z_2 - z_4) + x_2(z_4 - z_1)$$
$$c_4 = x_3(z_2 - z_1) + x_2(z_1 - z_3) + x_1(z_3 - z_2)$$
$$d_1 = x_4(y_3 - y_2) + x_3(y_2 - y_4) + x_2(y_4 - y_3)$$
$$d_2 = x_4(y_1 - y_3) + x_1(y_3 - y_4) + x_3(y_4 - y_1)$$
$$d_3 = x_4(y_2 - y_1) + x_2(y_1 - y_4) + x_1(y_4 - y_2)$$
$$d_4 = x_3(y_1 - y_2) + x_1(y_2 - y_3) + x_2(y_3 - y_1)$$

The method used weighted residuals in the Galerkin approach and was then applied to the differential equation, (2), where the integrations were performed over the element domain V .

$$\int_V N_n\left(\frac{\partial}{\partial x}\left(\frac{\partial H}{\partial x}\right) + \frac{\partial}{\partial y}\left(\frac{\partial H}{\partial y}\right) + \frac{\partial}{\partial z}\left(\frac{\partial H}{\partial z}\right)\right)dV - \int_V N_n\left(j\omega\mu\sigma - \mu\varepsilon\omega^2\right)HdV = 0$$

In the compact matrix form, they are:

$$[M + K]\{H\} = 0 \quad (5)$$

$$M = \left(j\omega\mu\sigma - \mu\varepsilon\omega^2\right)\int_V N_nN_mdV = \frac{\left(j\omega\mu\sigma - \mu\varepsilon\omega^2\right)V}{20}\begin{bmatrix} 2 & 1 & 1 & 1 \\ 1 & 2 & 1 & 1 \\ 1 & 1 & 2 & 1 \\ 1 & 1 & 1 & 2 \end{bmatrix} \quad (6)$$

$$K = \int_V\left(\frac{\partial N_n}{\partial x}\frac{\partial N_m}{\partial x} + \frac{\partial N_n}{\partial y}\frac{\partial N_m}{\partial y} + \frac{\partial N_n}{\partial z}\frac{\partial N_m}{\partial z}\right)dV$$

$$= \frac{1}{36V}\begin{bmatrix} b_1b_1 + c_1c_1 + d_1d_1 & b_1b_2 + c_1c_2 + d_1d_2 & b_1b_3 + c_1c_3 + d_1d_3 & b_1b_4 + c_1c_4 + d_1d_4 \\ & b_2b_2 + c_2c_2 + d_2d_2 & b_2b_3 + c_2c_3 + d_2d_3 & b_2b_4 + c_2c_4 + d_2d_4 \\ & & b_3b_3 + c_3c_3 + d_3d_3 & b_3b_4 + c_3c_4 + d_3d_4 \\ Sym & & & b_4b_4 + c_4c_4 + d_4d_4 \end{bmatrix} \quad (7)$$

For one element containing 4 nodes, the FEM approximation is a 4×4 matrix. With *n* nodes, the system is an *n*×*n* matrix.

C. Boundary Conditions and Simulation

The boundary conditions applied included a zero intensity magnetic field at the OHGW, 22-kV power lines, and the ground. For the boundary conditions at the outer perimeters of 115-kV power lines are given in Table I and the current in the line was 855 A [11]. The properties of materials used in this simulation are given in Table II [12]. The permittivity of free space (ε_0) is 8.854×10^{-12} F/m and the permeability of free space (μ_0) is $4\pi\times10^{-7}$ H/m.

TABLE I. THE BOUNDARY CONDITIONS FOR THE 115 KV CABLE

The surface of the conductor	Magnetic Field (μT)
115 kV phase A1	$601.8967\angle 86.2935^\circ$
115 kV phase A2	$604.3222\angle -86.6029^\circ$
115 kV phase B1	$599.8715\angle -74.0822^\circ$
115 kV phase B2	$600.0587\angle 85.7260^\circ$
115 kV phase C1	$602.2586\angle -84.0437^\circ$
115 kV phase C2	$600.2544\angle 85.3268^\circ$

TABLE II. PROPERTIES OF MATERIALS IN THE SIMULATION

Description	Electrical Conductivity (σ, S/m)	Relative Permittivity (ε_r)	Relative Permeability (μ_r)
Power Lines (copper)	3.8×10^7	3.5	1
Human Body	0.21	5.0	18.8
Steel	0.8×10^7	3.5	300.0
Air	0	1.0	1.0
Tower (cement)	1.0	1.0	1.0
Insulators (polyester)	0.1	1.17	8.0

D. Shielding the Magnetic Field

Shielding is generally done at the origin of the magnetic field. For example, this may be on high voltage transmission lines or at the location of devices affected by electromagnetic fields, such as computers or electronic devices. Two popular shielding methods are available, a flux shunting mechanism, and an induced current shielding mechanism [13-14]. This work focuses on magnetic protection using an induced current shielding mechanism since the blocking or reduction of magnetic

fields by this mechanism uses highly conductive materials such as silver, copper, and aluminum, among others. This mechanism occurs when the conductor material is placed in a changing electromagnetic field. The result is an induction of an electric field in the conductor material according to Faraday's law. The electric field formed in this conductor material causes an electric current that flows on the conductor's surface. This induced current is called an eddy current, which creates a magnetic field to counteract the original magnetic field. The magnetic field in this area is reduced as shown schematically in Fig.5. The advantage of blocking the magnetic field using this mechanism is that it can be accomplished using a small magnetic object. The disadvantage of using this mechanism is that the reflection coefficient and electromagnetic absorption are low.

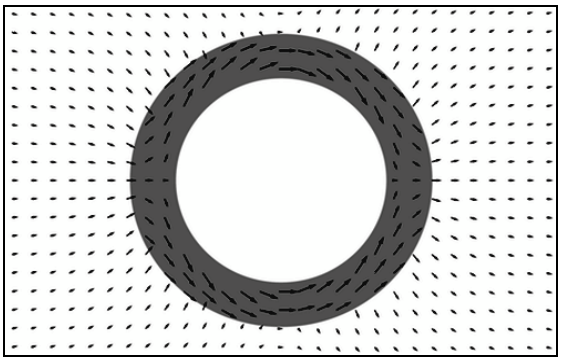

Figure 5. Induced current shielding mechanism

Proper shielding will reduce the intensity of the magnetic field in the shielded area. Shielding efficiency (SE), which is determined by the attenuation ratio of a magnetic field, when a magnetic field is emitted from a magnetic field source, measures the magnetic field strength at one point. If there are no magnetic objects in the area, then the object is blocked and the magnetic field intensity measured at the same point of observation. Again, the above definition is written as a mathematical equation.

$$SE(dB) = 20log\left[\frac{H_{unshield}}{H_{shield}}\right] \quad (8)$$

Materials that attenuate the magnetic field will depend on the skin depth (δ) as in (9).

$$\delta = \sqrt{\frac{2}{\omega\mu_0\mu_r\sigma}} \quad (9)$$

In this study, we introduce four types of materials for shielding magnetic fields, aluminium, steel, 80% Ni-Fe μ-metal, and Fair Rite – Type 76 Ferrite. Electrical conductivity and magnetic permeability values are shown in the TABLE III [15-16], where the entire body is covered to a depth of 5 mm.

TABLE III. PROPERTIES OF SHIELDING MATERIALS

Material	Conductivity (σ) S/m	Relative Permeability (μ_r)	Skin Depth (δ) m
Ferrite	2	10,000	0.503
Aluminum	3.8×10^{7}	1	1.15×10^{-2}
Steel	1×10^{7}	500	1×10^{-3}
80% Ni-Fe μ-metal	1.64×10^{6}	15,120	4.52×10^{-4}

IV. RESULT AND DISCUSSION

Finite element simulation was done using MATLAB for calculation of magnetic field dispersion. MATLAB was used due the simplicity of its approach to the simulation. The simulation results included contour zooms of magnetic field distribution through the cross-sectional volume of the working domain, graphical representation of magnetic field strength, and graphical representation of the magnetic field strength in a human body near the transmission system. These are presented in Figs.6, 7and 8, respectively. In the simulation, a model of a 180 cm tall human body was exposed to the magnetic effects of a 50 Hz overhead power transmission line. The power line and human were 12 m above the ground.

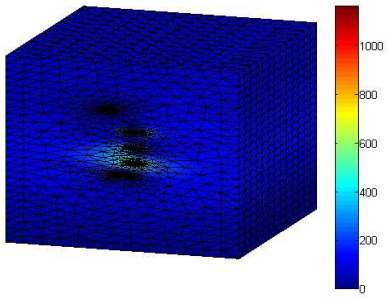

Figure 6. Magnetic field distribution (μT)

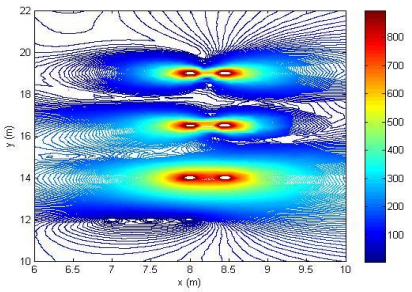

Figure 7. Magnetic field contours zoom (μT) at a cutaway position of the center of the operator body

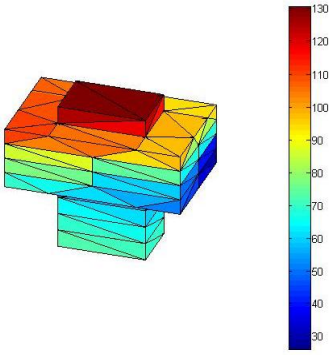

Figure 8. Magnetic field distribution in a human body (μT)

In Figs. 6 and 7, show the distribution of the magnetic field in the power transmission lines. It can be seen that the magnetic field is very strong near the surface of the 115 kV conductor. Fig. 8 shows the effect of the magnetic field on the human body. Average and maximum values of the magnetic field of a human were 70.92 μT, and 130.46 μT, respectively. It was found that the magnetic field was strongest at the head of the human body because it is nearer to the conductor. This value exceeds acceptable safety limits and is hazardous to humans. The International Commission of Non-Ionizing Radiation Protection [17], set the level of magnetic field safe to the general public as not greater than 100 μT over a 24 hours period, and it must not exceed 500 μT for a work day. Therefore, human beings must be protected against the effects of magnetic fields near transmission lines. The results of the simulation of magnetic protection are shown in Figs. 9- 12. The simulation results of magnetic field protection and SE values are shown in TABLE IV. Figs. 9-12, show magnetic field contours and their distribution in the human body (μT) at a cutaway position of the center of the operator body when ferrite, aluminium, steel, and 80% Ni-Fe μ-metal materials are used for protection, respectively. At the bottom left, the shape of a human body is depicted. The magnetic field is less prominent because of the shielding materials used.

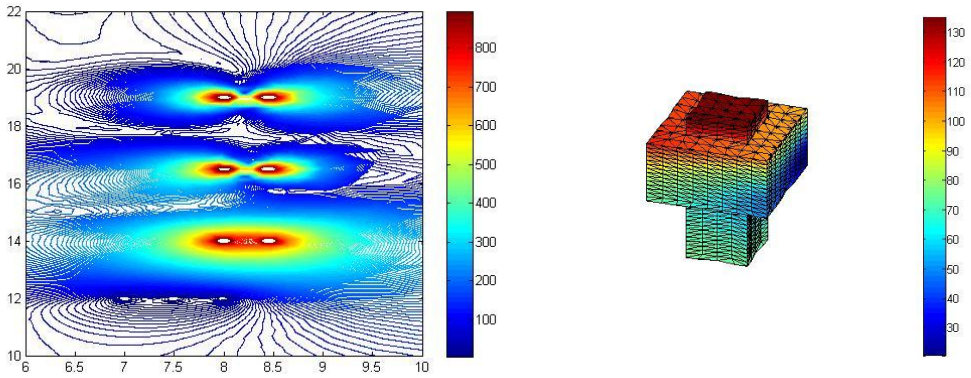

Figure 9. Magnetic field contours and distribution at the center of a human body (μT) using ferrite materials for shielding

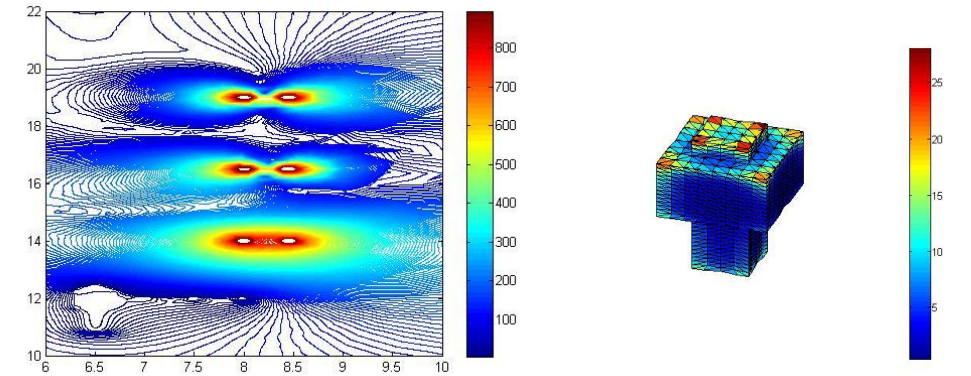

Figure 10. Magnetic field contours and distribution at the center of a human body (μT) using aluminum materials for shielding

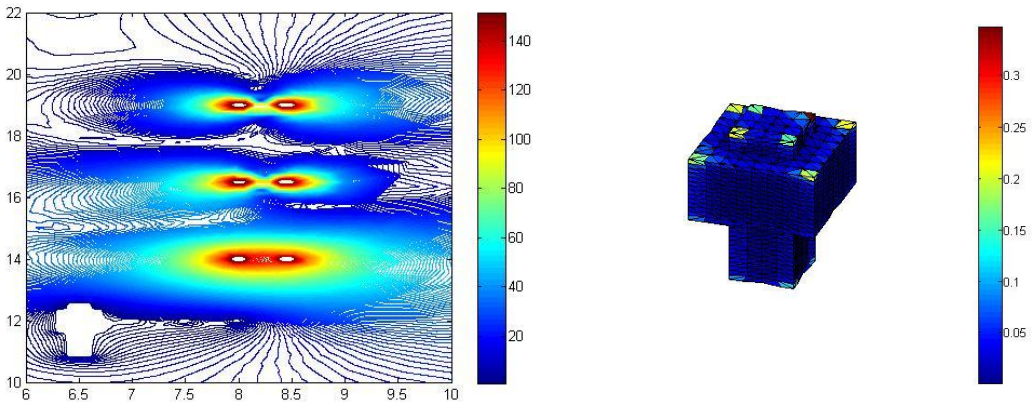

Figure 11. Magnetic field contours and distribution at the center of a human body (μT) using steel materials for shielding

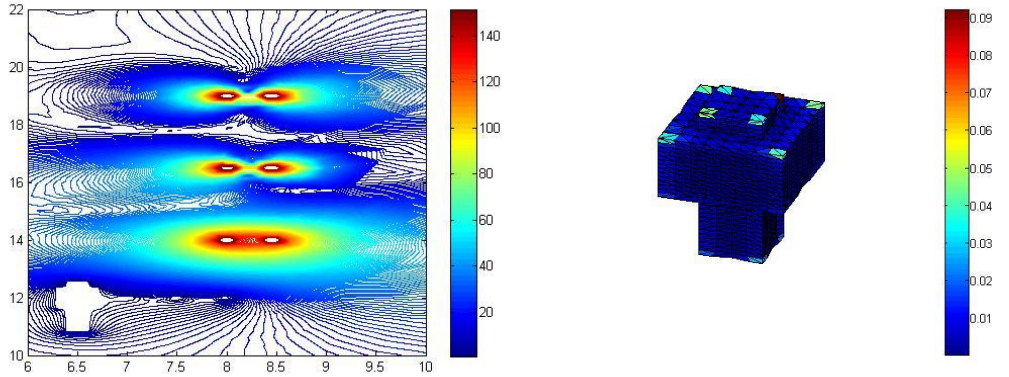

Figure 12. Magnetic field contours and distribution at the center of a human body (μT) using 80% Ni-Fe μmetal materials for shielding

TABLE IV. MAGNETIC FIELD IN A HUMAN BODY

Shielding materials	Maximum magnetic field in human (μT)	Average magnetic field in human (μT)	Shielding efficiency (SE,dB)
No shield	130.46	70.92	0
Ferrite	130.2254	70.3268	0.07
Aluminium	27.9704	4.2522	24.44
Steel	0.3464	0.0105	76.59
80% Ni-Fe μ-metal	0.0920	0.0021	90.57

This work shows the distribution of a magnetic field that affects the operator of a 22 kV transmission line. Its power is cut, but it is affected by a nearby 115 kV transmission line, resulting in an internal magnetic field. It is necessary to reduce this magnetic field using ferrite, aluminium, steel, 80% Ni-Fe μ-metal as shown in Figs. 9-12, with an induced current shielding mechanism. TABLE IV shows the maximum and average magnetic fields in a human body, and the shielding efficiency (SE) obtained with materials that affect magnetic attenuation such as aluminium, steel, and 80% Ni-Fe μ-metal. The results comply with the International Commission on Non-Ionizing Radiation Protection (ICNIRP), and the 80% Ni-Fe μ-metal yielded the best protection. Its high conductivity and magnetic permeability reduce the magnetic field as a function of its skin depth as is shown in (9).

V. CONCLUSION

This work studied the magnetic field distribution caused by a 115 kV power transmission line hung over a 22 kV line on the same tower. Computer simulation based on a FEM in the time-harmonic mode with the appropriate graphical representations of magnetic fields was conducted. The shield was based on the induced current shielding mechanism. Four materials were used to shield the magnetic field: ferrite, aluminium, steel, 80% Ni-Fe μ-metal. Simulation results showed that the 80% Ni-Fe μ-metal offers the best magnetic protection.

ACKNOWLEDGMENT

This work was supported by the School of Electrical Engineering, Institute of Engineering, Suranaree University of Technology.

REFERENCES

[1] N. A. Demerdash and D. H. Gillott, "A new approach for determination of eddy current and flux penetration in nonlinear ferromagnetic materials," *IEEE Transactions on Magnetics*, vol. 74, pp. 682-685, 1974.

[2] P. Pao-la-or, A. Isaramongkolrak, and T. Kulworawanichpong, "Finite element analysis of magnetic field distribution for 500-kV," *Power Transmission Systems Engineering Letters*, no.1, vol. 18, pp .1-9, 2010.

[3] P. Pao-la-or, "Study of magnetic field shielding roof of cabin electricity authority resulting in operators working," *WSEAS* Transaction *on Power System*, vol. 10, no. 6, pp 163172, 2011.

[4] A. Bunmat and P. Pao-la-or, "Analysis of magnetic field effects operators working a power transmission line using 3-D finite element method," in *Proc. 18th International Conference on Electrical Machine and System (ICEMS)*, Oct. 25-28, Pattaya City, Thailand , 2015, 1187-1191.

[5] S. Vacharakup, M. Peerasaksophol, T. Kulworawanichpong, and P. Pao-la-or, "Study of natural frequencies and characteristics of piezoelectric transformers by using 3-D finite element method," *Applied Mechanics and Materials*, vols. 110-116, 2012, pp .61-66.

[6] M. V. K. Chari and S. J. Salon, "Numerical methods in electromagnetism," *Academic Press*, USA, 2000.

[7] M. Weiner, "Electromagnetic analysis using transmission line variables," *World Scientific Publishing*, Singapore, 2001.

[8] C. Christopoulos, "The transmission-line modeling method: TLM," IEEE Press, USA, 1995.

[9] T. W. Preston, A. B. J. Reece, and P. S. Sangha, "Induction motor analysis by time-stepping techniques," *IEEE Transactions on Magnetics*, vol. 24, no. 1, 1988, pp. 471-474.

[10] B.T. Kim, B.I. Kwon, and S. C. Park, "Reduction of electromagnetic force harmonics in asynchronous traction motor by adapting the rotor slot number," *IEEE Transactions on Magnetics*, vol. 35, no. 5, 1999, pp. 3742-3744.

[11] P. Pin-anong, "The electromagnetic field effects analysis which interfere to environment near the overhead transmission lines and case study of effects reduction," [M.Eng. thesis], School of Electrical Engineering, Department of Electrical Engineering, King Mongkut's Institute of Technology Ladkrabang, Bangkok, Thailand, 2002.

[12] A. Cipollone, A. Fabbri, and E. Zendri, "Techniques for shielding underground power lines to minimize the exposure to

elf magnetic field in residential areas," *International Symposium on Electromagnetic Compatibility*, Sorrento, Sept. 2002.
[13] H. Uetake, N. Hirota, Y. Ikezoe, and K. Kitazawa, "Magnetic-field simulation for shielding from high magnetic fields," *Journal of Applied Physics*, vol.91, no.10, 2002, pp. 6991-6993.
[14] K. Wassef, V. Varadan, and K. Varadan, "Magnetic field shielding concepts for power transmission lines," *IEEE* Transactions *on Magnetics*, vol. 34, no. 3, 1998, pp. 649-654.
[15] S. Shahsavari and H. Sarfi, "Study of the system characteristics on the performance of the sheet metal electromagnetic forming," *International Journal of Electrical and Electronic Engineering & Telecommunications*, vol. 6, no. 1, 2017, pp. 1-11.
[16] M. D'Amore, E. Menghi, and M. S. Sarto, "Shielding techniques of the low-frequency magnetic field from cable power lines," in *Proc. IEEE International Symposium on Electromagnetic Compatibility*, vol. 1 , 2003, pp. 203-08.
[17] International Commission of Non Ionizing Radiation Protection (ICNIRP), Guidelines for Limiting Exposure to Time-Varying Electric, Magnetic and Electromagnetic Fields (up to 300 GHz)," Health Phys., vol. 74, no. 4, 1998, pp. 494-522.

Padej Pao-la-or received his B. Eng. (1998), M. Eng. (2002) and D. Eng. (2006) in Electrical Engineering from Suranaree University of Technology, Thailand.

He is an Associate Professor in the School of Electrical Engineering, Institute of Engineering, Suranaree University of Technology, Nakhon Ratchasima, Thailand. His fields of research interest include a broad range of power systems, finite analysis, optimization and artificial intelligence, electromagnetic field, electrical machinery and energy conversion. He joined the school in December 2005 and is currently a member in Power System Research, Suranaree University of Technology.

Arak Bunmat is a pursuing a doctoral degree in the School of Electrical Engineering, Institute of Engineering, Suranaree University of Technology, Nakhon Ratchasima, Thailand.

He received his B.Eng. (2009) and M. Eng. (2013) in Electrical Engineering from Suranaree University of Technology, Thailand. His fields of research interest include a broad range of power systems, electrical drives, FEM simulation and artificial intelligence techniques.